Bog iron ore from Lowland Point, St Keverne, Lizard, Cornwall

P.W. Scott [1,3], P.J. Ealey [2] and G.K. Rollinson [1]

Scott, P.W., Ealey, P.J. and Rollinson, G.K. 2011. Bog iron ore from Lowland Point, St Keverne, Lizard, Cornwall. *Geoscience in South-West England*, **12**, 260-268.

Concretionary masses of bog iron ore occur at the contact of two clayey silts in the low cliffs at Polcries, Lowland Point, Lizard. The lower clayey silt rests on weathered gabbro. The area containing the ore is characterised by very large bounders of gabbro on the foreshore. The ores have a complex mineralogy, which has been investigated by optical microscopy, X-ray diffraction, scanning electron microscopy and QEMSCAN®. Although goethite is present, most of the Fe occurs as poorly crystalline or amorphous pisoid shaped masses of oxides / hydroxides often associated with variable amounts of silica and/or alumina. Variable amounts of poorly crystalline or amorphous Mn oxides / hydroxides are also found, similarly mixed with variable amounts of silica and/or alumina. There is partial segregation of the Fe and Mn. The ore forms a matrix to angular quartz and other detrital minerals most likely of loessic origin together with some fragments of minerals from the gabbro.

The clayey silts have quartz as the dominant mineral, the clay mineral components being kaolinite, illlite and a poorly crystalline mixed layer illite-smectite. They are interpreted as transitional to loess found further to the south and possibly accumulated in a lagoonal setting. The very large gabbro boulders, which rest on top and within the lower clayey silt, are probably the remains of a periglacially degraded cliff. Transport of the Fe and Mn was by groundwater flow with the metal source being from deep weathering of the gabbro. Precipitation of the Fe and Mn took place in response to either oxidation, or more likely, an increase in pH due to sea water or salt spray percolating into the vadose zone, the lower clayey silt acting as an impermeable barrier. Partial segregation of Fe and Mn is due to fluctuations in Eh and pH causing differential dissolution and precipitation. This is the first reported occurrence of bog iron ore in Cornwall.

[1] Camborne School of Mines, University of Exeter, Tremough Campus, Penyrn, Cornwall, TR10 9EZ , U.K.
[2] 8 Minster Fields, Manaccan, Helston, Cornwall, TR12 6JG, U.K.
[3] Peter W. Scott Ltd, Kinloss, Port Navas, Falmouth, Cornwall TR11 5RL, U.K.
(E-mail: p.w.scott@ex.ac.uk).

Keywords: Cornwall, Lizard, Lowland Point, bog iron ore, manganese ore, gabbro, loess.

Introduction

Bog iron ores are sedimentary concentrations of iron oxides and hydroxides found in soils, marshes and peats in a habitat of swamps, lakes and sluggish streams of recently glaciated terrains (Stanton, 1972). They can vary from diffuse or localised, soft and spongy textured masses, often associated with a lot of plant debris, to hard concretionary or layered deposits. The ore was used as an early source for iron production in pre-industrial Britain, being particularly common in upland areas in Scotland, northern England and Wales.

At Lowland Point on the Lizard, Cornwall, a localised occurrence of bog iron ore is present as concretionary masses in the low cliffs adjacent to the beach. Small lumps of the ore, eroded from the cliffs, are also found on the foreshore. This paper describes the geological setting of the iron ore, its chemistry and mineralogy, and provides a model for its genesis. There is no evidence that it provided an historic source of ore for smelting.

Geological setting

Lowland Point (SW 804196), on the east side of the Lizard Peninsula, Cornwall, is a small promontory to the south-west of the offshore Manacles Rocks and to the north-east of Coverack (Figure 1). It is unusual for the Lizard in that low cliffs only a few metres high are present directly facing the sea. These are backed by a wide terrace, referred to as a raised beach by Budge (1842) and Flett (1946), with an older much higher palaeo-cliff behind (Figure 2). The iron ore is found in a bay 200 m to the north of the most easterly part of Lowland Point, stretching for 100 m or so towards Dean Quarry. The area is marked as Polcries on the 1:25,000 Ordnance Survey map.

The bedrock in the area is the Crousa Gabbro (Floyd *et al*,. 1993), which is exposed in cliffs and on the foreshore for the whole distance from Coverack to Porthoustock. The same gabbro extends inland for several kilometres beneath a relatively flat plateau of partly improved grazing land, along with much unimproved and undrained heathland on which large residual boulders of gabbro, known locally as 'crusairs', can be found. The plateau and gently sloping surfaces of the gabbro behind the palaeo-cliff are deeply weathered for up to

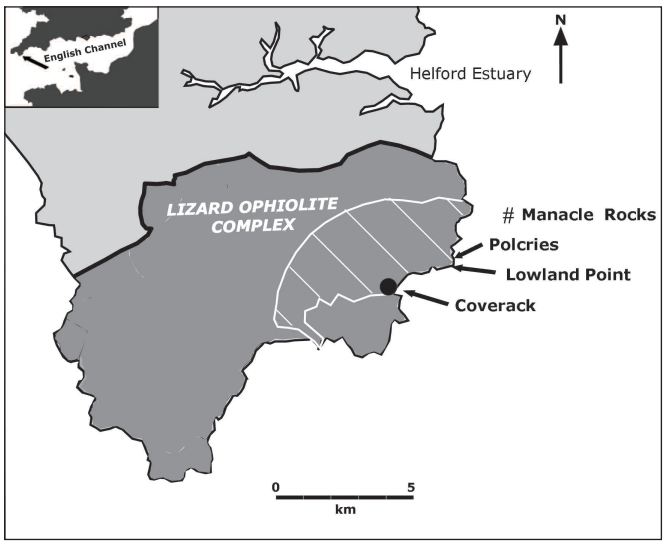

Figure 1. *Location map of Lowland Point, Lizard, Cornwall. The diagonal lined area shows the extent of gabbro within the ophiolite complex. Inset map shows the location of the Lizard area.*

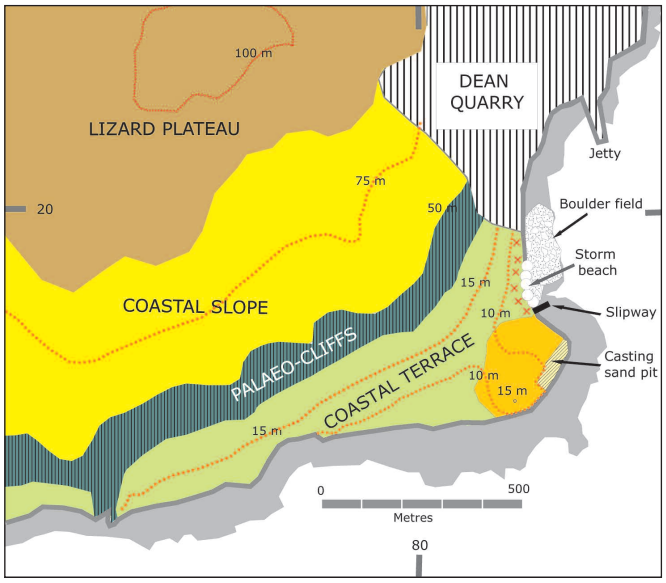

Figure 2. *Location of bog iron ore at Lowland Point, along with geomorphological setting. The red line xxxxx shows the length of the present low cliff with bog iron ore* in situ. *The ore is partly beneath the storm beach. The extent of the loess behind the casting sand pit, from where loess was formerly extracted, is shown in orange.*

15 m or more, as can be seen in Dean Quarry, just to the north of Lowland Point.

The iron ore occurs in an upper clayey silt present at the base of the soil horizon in the low cliffs (Figures 3, 4a and Table 1) at the contact with a separate lower clayey silt. It forms isolated semi-hard to very hard orange brown to dark brown concretionary masses between the clayey silts. Separate fragments of the harder ore are found on the foreshore. The masses vary in size, typically being a few 10s of centimetres horizontally across by 10-20 cm thick. *In situ*, they sometimes partly merge to form a larger more elongate horizontal layer up to 1-2 m in length at the interface between the upper and lower clayey silt. The ore also occurs as masses in between boulders of gabbro (Figure 4b), some of which appear to have been broken, presumably by frost, prior to development of the ore mass. The ore is also found adhering to gabbro boulders, and some boulders on the foreshore away from the cliff have the weathered remains of the iron ore attached (Figure 4c), the top of the attached ore forming a distinct horizontal line at the same level as the contact between the upper and lower clayey silts.

On the foreshore immediately in front of the *in situ* iron ore the gabbro boulders are much larger than those of the surrounding area (Figure 3), with a clear line separating the boulder sizes. These large boulders are seen to rest on, or are sunk into, the lower silty clay, which in turn rests on soft weathered gabbro. The latter, being visible only close to the low water mark, is in contrast to the more usual, hard, unweathered, rocky exposures of gabbro of the foreshore in the surrounding area. This suggests a spatial and age relationship between the iron ore, the lower silty clay, the large boulders and the weathered gabbro.

The upper clayey silt at the base of the soil profile is grey brown and structureless with some small pebbles in addition to the larger boulders (Table 1). The lower clayey silt is brownish yellow with polygonal greyish fractures. There is some water seepage in the cliff between the two clayey silts. The clayey silts pass laterally southwards into a friable, almost clay-free loess at Lowland Point described by Ealey and James (2011), who consider it to be of Weichselian/Devensian age.

The Soil Survey Memoir at the location of the iron ore (Staines, 1984) labels the soil as Polcoverack Series, described as stoney, fine loamy cambic gley soils in thick gabbroic head or over weathered *in situ* gabbro. Adjacent, and closer to Lowland Point, Gwavas Series soils are described as *"stoneless coarse gleyic brown earths in thick (>1 m) loess, either over.....gabbro....or over a raised beach deposit"*. The Gwavas Series soils fits better with the observed stratigraphy of the sediments containing the iron ore. Ferri-manganiferous soft concretions are mentioned by Staines (1984) as present in the B soil horizon of both soil types.

The foreshore around Lowland Point also has boulders of a haematite / goethite iron ore from the coaster *Ocklinge*,

Figure 3. *Area of foreshore and land to the north of Lowland Point with Dean Quarry in background. The bog iron ore is found in the low cliff in the middle ground where the large boulder field meets the land. The ore is only found in the cliff and foreshore within the large boulder field.*

Figure 4. *Field photographs of bog iron ore occurrences. (**a**). Bog iron ore* in situ *in low cliff. The ore (dark brown discontinuous layer) is at the base of the upper grey brown clay to the right of the hammer and below the large boulder. (**b**). Large mass of bog iron ore between and enclosing gabbro boulders on foreshore. (**c**). Part of a large boulder (approx. 6 m³) with adhering black residual iron ore. Note the sharp horizontal line marking the base of the ore. This corresponds to the same level as the contact between the upper and lower clayey silt. Coin 28 mm diameter (circled).*

0 – 15 cm	Unit 1a. Dark brown soil with upper vegetation cover, charged with small pebbles, often rounded and <5 cm.
15 – 65 cm	Unit 1b. Grey-brown (7.5YR 5/2) structureless clayey silt with large boulders up to 1 m plus and minor bee burrows. Bottom 10 cm with smaller clasts.
Iron ore horizon	
65 – 105 cm+	Unit 2. Brownish yellow clayey silt (10YR 6/6) with decimetre polygonal greyish fractures with deeper brown lenses of granular gabbroic debris.

Table 1. *Measured section of cliff showing position of iron ore.*

wrecked in 1932 whilst on route from Bilbao to Newport (Bates and Scolding, 2000). This iron ore has a very different appearance to the bog iron ore described in this paper.

Analytical procedures

Five samples were collected from different iron ore masses. The overall chemical composition was determined by X-ray fluorescence spectrometry (XRF) using a Bruker S4 Pioneer and a standardless procedure. Samples were dried and pulverised in a tungsten carbide mill and prepared as pressed powders in borate jackets. This analytical method enables the major, minor and trace elements to be recognised and provides a semi-quantitative analysis. It does not give an accurate analysis, but the data are precise within a similar set of samples and shows up any variation in composition. The loss on ignition (LOI) was separately determined by calcining a sample at 1000°C for 30 minutes.

Initial recognition of the minerals present in the samples was made by powder X-ray diffraction using a Siemens D5000 θ/θ diffractometer, CuKα radiation, and scanning from 2-70°2θ with count time of 2 sec for each 0.02°2θ step. Minerals were identified using Bruker EVA software and reference to published data in the ICDD files. Further mineralogy and petrography were determined by optical microscopy of polished thin sections and polished blocks in transmitted and reflected light, by examination in a Jeol JSM-5400LV scanning electron microscope (SEM), using back-scatter detector mode with EDS analyser, and by using an Intellection QEMSCAN® 4300. The latter is an automated SEM with four energy dispersive spectrometers and an electron backscatter detector (Gottlieb *et al.*, 2000; Pirrie *et al.*, 2004). The whole area of a 30 mm polished block was scanned at 10 µm intervals (Fieldscan measurement mode), with 1000 X-ray counts collected at each point. Discrimination between the X-ray spectra from different phases in the sample enables a 'mineral map' of the whole surface to be obtained. Data was processed using procedures discussed in Rollinson *et al.* (2011). In addition, the particle size distribution of the phases was determined.

The particle size distribution of the clayey silt above and below the iron ore horizon was determined by wet sieving to 250 µm to remove coarse size fractions including gabbro clasts, and then by the Malvern laser Mastersizer Micro. A <2 µm fraction was separated by settling after dispersion of the <63 µm fraction. The mineralogy of the <250 µm fraction was determined by XRD, and the clay mineralogy of the <2 µm fraction was determined by XRD using a pressed-powder (i.e. partially orientated) sample and scanning from 2-30°2θ, using the same operating conditions as above.

CHEMISTRY

The semi-quantitative chemical analyses of the iron ore samples are given in Table 2. Fe_2O_3, SiO_2 and Al_2O_3 are present in large but variable amounts. Fe_2O_3 (26-42%) broadly shows an inverse relationship with SiO_2 (30-42%) and Al_2O_3 (9-12%). MnO is present in significant, but variable (1-7%) amounts. High amounts of MnO broadly correspond to lower amounts of Fe_2O_3 and vice versa. Other minor elements present are MgO, CaO, K_2O, Na_2O, TiO_2, P_2O_5, S and Cl. The latter two, along with some Na_2O, MgO and CaO could be accounted for by the presence of chlorides and sulphates from sea-water in the pores of the samples. The loss on ignition is high and variable (8.6 – 11.6%).

The list of trace elements (Table 2) shows that Ba (200-900 ppm) is a significant component. V (300-450 ppm), Cr (160-220 ppm), Co (190-540 ppm), Ni (90-250 ppm), Zn (110-200 ppm) and Zr (190-300 ppm) are also present in amounts greater than 100 ppm and sometimes much more. There are small amounts of Cu (50-60 ppm), Rb (60-70 ppm), Sr (70-110 ppm), Y (10-20 ppm) and Br (60-70 ppm). The latter most likely is from salts in pores in the samples with a sea-water origin rather then as a component within the iron ore.

Sample No	3/10	4/10	5/10	6/10	7/10
%					
SiO_2	31.24	41.68	29.69	32.87	36.97
TiO_2	0.45	0.71	0.42	0.50	0.63
Al_2O_3	12.32	12.27	10.94	9.54	12.24
Fe_2O_3	33.60	27.45	40.32	42.03	28.44
MgO	1.24	1.60	1.14	1.05	1.42
MnO	5.06	3.60	2.26	0.97	6.54
CaO	0.56	1.01	0.64	0.67	0.78
Na_2O	0.87	0.98	0.84	0.61	0.93
K_2O	1.34	1.46	1.17	1.17	1.42
S	0.11	0.05	0.06	0.05	0.08
Cl	0.31	0.18	0.26	0.04	0.35
P_2O_5	1.10	0.17	0.46	0.44	0.18
LOI	11.55	8.62	11.59	9.87	9.77
Total	99.75	99.78	99.79	99.81	99.75
ppm					
V	300	300	447	380	320
Cr	162	209	204	208	224
Co	339	346	320	192	542
Ni	163	154	94	64	247
Cu	54	61	48	57	55
Zn	203	154	138	110	172
Br	24	23	33	nd	nd
Rb	67	71	63	62	69
Sr	96	95	109	75	93
Y	19	20	10	14	17
Zr	195	299	194	264	284
Ba	851	560	430	210	901

LOI – loss on ignition. nd – below detection limit.

Table 2. *Chemical composition of iron ore samples.*

MINERALOGY AND PETROGRAPHY OF IRON ORE

The hard iron ore masses have an orange-brown to brown surface and appear porous. Fresh broken surfaces are dark brown to black and sometime finely mottled with a rounded pisolitic-like structure (Figure 5a). Quartz, goethite, K-feldspar and plagioclase are identified from XRD as present in the ore. The traces, however, have a high background suggesting an abundance of poorly crystalline or amorphous material. Ferrihydrite, which is a very poorly crystalline species with broad peaks may also be present, although its reflections overlap largely with goethite. No manganese minerals could be identified.

Microscopically, the ore is made up dominantly of 10-50 µm angular quartz grains (90%+), along with much smaller amounts of similar sized K-feldspar, plagioclase and mica grains (<10%) (Figure 5b) in a fine-grained matrix. The grains are discrete and separated. There are occasional larger plagioclase and pyroxene / amphibole grains up to around 0.5 mm. In addition there is a wide range of other mineral grains, including ilmenite, zircon, and sphene, usually much smaller than the quartz and feldspar and present in very small amounts (<0.1%).

In reflected light, the matrix mostly has a very low diffuse reflectivity indicating it is a very fine-grained, although a few higher reflecting areas, probably of more crystalline goethite, are also present (Figure 5c). With the SEM in back-scatter mode, the matrix is seen to be very variable, with patches of different compositions (Figure 5d) at various scales, resulting from areas having varying combinations of Fe, Mn, Si and Al in varying amounts. No distinct grain or crystal boundary exists between these different compositions within the matrix.

Data from the QEMSCAN® in Fieldscan measurement mode on one sample (3/10) enables more details of the texture and composition of the grains and matrix to be obtained. The complete range of compositions is given in Table 3, along with percentages of each phase. Named minerals are listed where the composition identified by the energy dispersive analysis is considered to be unambiguous. These correspond almost entirely to the mineral grains (e.g. quartz, K-feldspar, zircon, ilmenite) rather than the matrix. Element assemblages (e.g. Fe-Si-Al oxide, Mn-Fe-Si oxide) correspond to the range of compositions found within the matrix. Figure 6 shows a field of view of part of the sample with the compositions identified. Figure 7 shows the whole of the surface of the polished block, colour shaded to pick out the Fe-dominant and Mn-dominant parts in the matrix.

The mineral grains can be grouped into three types: (a). Those typically very resistant to weathering and dissolution, and to be expected in loessic silts and/or mature soil horizons in a temperate climate (quartz, K-feldspar, muscovite). (b). Those more susceptible to chemical weathering and less commonly present in a mature soil horizon (plagioclase, pyroxene / amphibole, Fe mica), although they would be expected in a soil developing over gabbro bedrock. (c). Minerals of high specific gravity and resistant to chemical weathering (chromite, rutile / anatase, ilmenite, sphene, zircon, monazite, xenotime, apatite, topaz).

The matrix compositions show that Fe oxide, Mn oxide and mixed Fe – Mn oxide compositions are present, but these elements also occur in combination with varying amounts of Si and/or Al. Although goethite is recognised as a crystalline phase by XRD, the bulk of the matrix is assumed, therefore, to be at least poorly crystalline and/or amorphous. The Mn-rich compositions particularly must be very poorly crystalline or amorphous as no Mn minerals are identified by XRD.

The matrix texture is heterogeneous with irregular areas, 1-2 mm across rich in Fe – Si – Al oxides and Mn – Fe – Si oxides dominant. Areas of Fe oxides and Fe – Al oxides of a few 10s of µm in size up to 100 µm tend to be present within the Fe – Si – Al oxides. Areas of exclusively Mn oxide up to 100 µm, Mn – Fe – Al oxides up to 50 µm, and Fe – Mn oxides up to 100 µm, are found almost only within the Mn – Fe – Si oxide dominant areas. Fe – Mn oxides and Mn – Fe – Al oxide areas seem to be associated, as do the Fe oxide and Fe – Al oxide areas along with the Fe – Mn oxides to a lesser extent, being found together in clusters. Fe-rich oxide areas, without Mn, generally have developed separately from those containing Fe and Mn oxides. Si and Al are more randomly distributed both separately and together within the Fe-rich oxide and Fe – Mn rich oxide areas. Pyrite, chalcopyrite, barite, fluorite and Ca, Ca – Mg and Ca – Mg – Fe carbonate identified phases are present as a few isolated 10 µm or slightly larger areas.

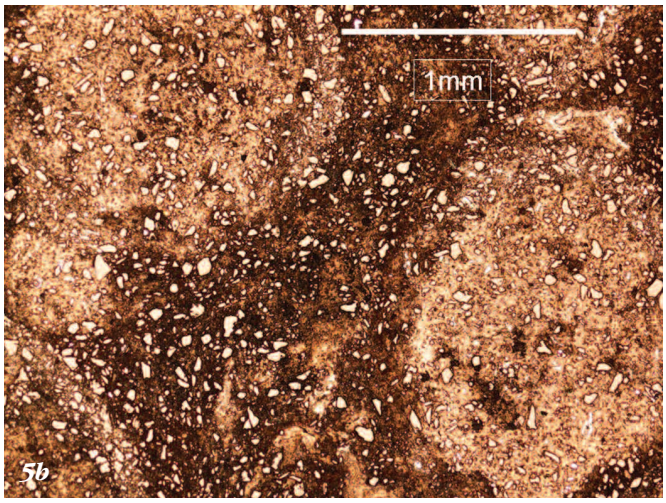

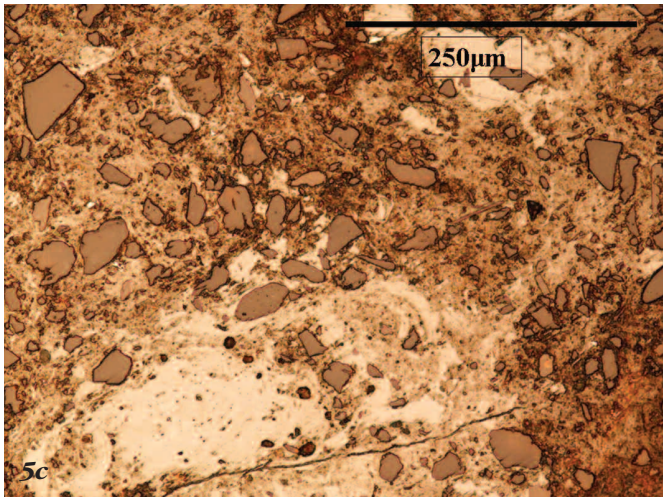

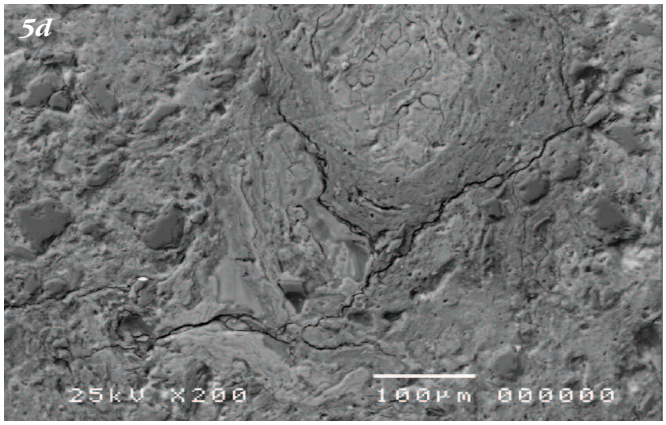

Figure 5. *Details of bog iron ore samples. (**a**). Sample of bog iron ore with dark brown to black fresh broken surface, brown surface weathering and pisolite-like porous structure. Coin 24 mm diameter. (**b**). Low magnification photomicrograph of polished surface of bog iron ore in reflected light showing small angular quartz along with other minor silicates in a matrix showing pisolitic texture. Lighter areas of matrix are variable mixtures of iron and manganese oxides and hydroxides. Darker matrix areas are more clay rich. (**c**). Photomicrograph of polished surface in plane polarised reflected light showing angular grains of low reflecting quartz in a matrix of variable reflectivity. Higher reflecting areas are more crystalline iron and/or manganese oxides/hydroxides, particularly goethite. Lower reflectivity areas are mixtures of low crystallinity iron and manganese oxides plus clay minerals. (**d**). SEM back scatter electron image of bog iron ore showing concentric and irregular structures within the matrix caused by varying amounts of Fe, Mn, Si and Al. For example, the centre of the concentric structure (upper centre) has a high Fe/Mn ratio with some Si and Al, with a high Mn/Fe ratio area and no Si and Al surrounding it.*

Mineral or elemental composition	Grain (G), matrix (M) or uncertain (?)	%
Quartz	G	9.18
K-feldspar	G	1.35
Plagioclase feldspar	G	1.18
Pyroxene / amphibole	G	1.45
Chromite	G	<0.01
Rutile / anatase	G	0.10
Ilmenite	G	0.08
Sphene	G	0.02
Muscovite	G	0.21
Zircon	G	0.01
Monazite	G	<0.01
Xenotime	G	<0.01
Apatite	G	<0.01
Topaz	G	<0.01
Pyrite	?	0.01
Chalcopyrite	?	<0.01
Fluorite	?	<0.01
Fe oxide or carbonate	M	0.87
Fe – Mn oxide	M	0.92
Fe – Si – Al oxide	M	51.64
Fe – Al oxide	M	0.52
Mn – Fe – Al oxide	M	0.40
Mn – Fe – Si oxide	M	29.83
K – Fe – Si – Al	M	1.38
Mn oxide	M	0.68
Kaolinite	M	0.15
Barite	?	<0.01
Ca, Ca – Mg and / or Ca – Mg – Fe Carbonates	?	0.01
Others	?	<0.01
Total		99.98

Table 3. *Mineral compositions in the iron ore identified using the QEMSCAN®. The mineral is identified where the energy dispersive spectrum is considered unambiguous. Otherwise the elemental composition is given. The oxides could also be variably hydrated. Under the conditions used for collection of the QEMSCAN® data, it is not possible to separate Ca-rich pyroxenes and Ca-rich amphiboles. Note: Percentages refer to this sample only. They vary within and between different masses of the ore.*

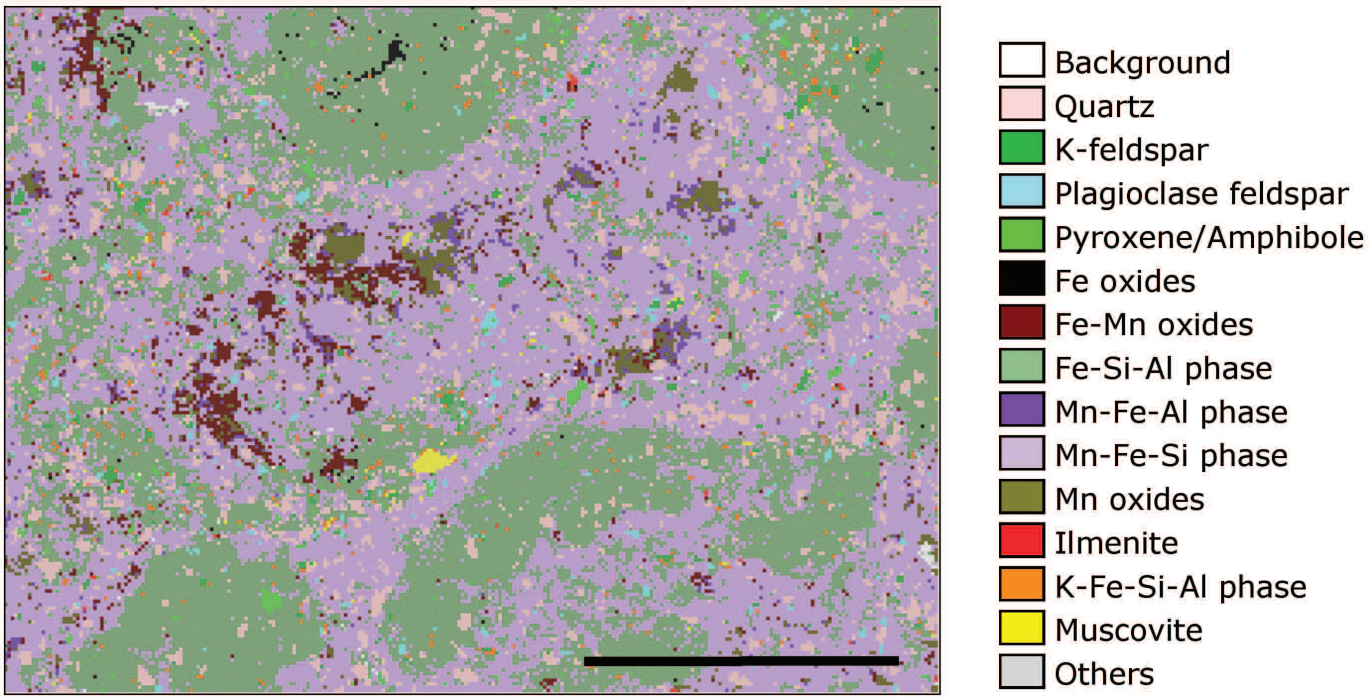

Figure 6. *QEMSCAN® high resolution false colour image of the texture and individual phases in the bog iron ore. The matrix is dominated by Fe-Si-Al and Mn-Fe-Si phases with lesser areas of Fe, Mn and Fe-Mn oxides. The matrix encloses grains of quartz, K-feldspar, plagioclase, pyroxene/amphibole, ilmenite and muscovite. The K-Fe-Si-Al phase probably represents original micas or clay minerals in the matrix. Scale bar = 1 mm.*

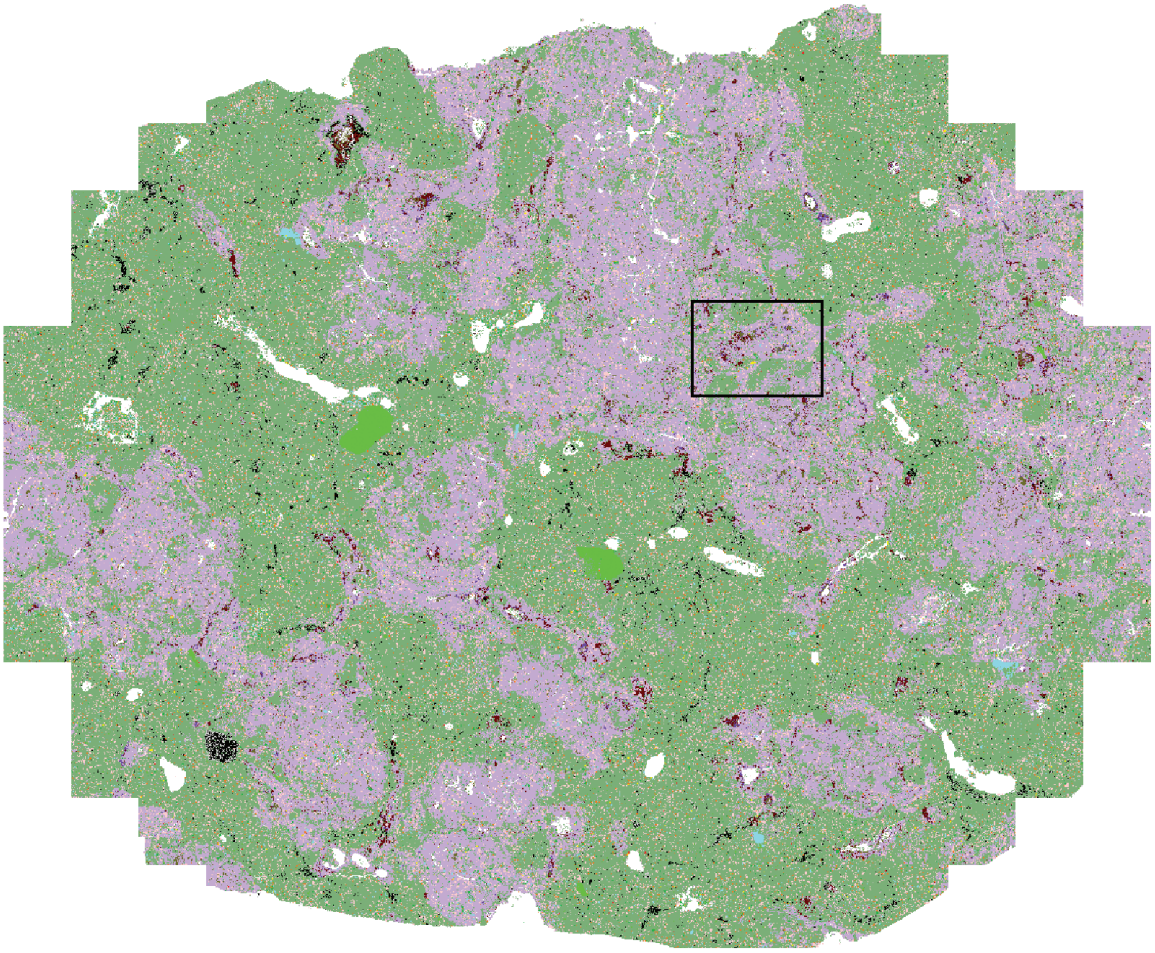

Figure 7. *QEMSCAN® false colour image of the whole surface of a polished block of the bog iron ore (sample 3/10) showing the texture and the relative distribution of Fe-rich with Si and Al (dull green) areas without Mn and areas rich in both Mn and Fe along with Al and or Si (blue and purple). Small brown and black areas are Fe and Fe-Mn oxide respectively. Small blue areas are Mn oxides. Bright green areas are pyroxene or amphibole. Small bright blue areas are plagioclase, and white represents holes in the sample surface. Area of Figure 6 shown by rectangle. Width of field of view = 27 mm.*

Particle size distribution and mineralogy of upper and lower clayey silt

The particle size distributions of the <250 µm fractions of the clayey silt above and below the iron ore horizon are shown in Figure 8. Fine sand and silt dominate the distributions, but they are bimodal with a small increase in the <2 µm range, suggesting a very fine grained and probably disordered clay mineral assemblage. The mineralogy determined by XRD of the <250 µm fraction of both the upper and lower clayey silt is dominated by quartz. The XRD traces also indicate a few percent of plagioclase and hornblende in the upper clayey silt and a few percent of K-feldspar and plagioclase in the lower clayey silt.

The <2 µm clay fractions of the clayey silts differ in their compositions (Figure 9). The XRD profile of the upper one shows a low intensity very broad reflection from 6-9°2θ (9.8-14.7Å), suggesting the presence of a poorly crystalline random mixed layered illite-smectite mineral. In addition there is a small reflection at 12.4°2θ (7.14Å) for kaolinite. The <2 µm fraction of the lower clayey silt has well developed basal reflections for a mica clay mineral (illite?) and kaolinite, along with slightly elevated counts in the region 6-8°2θ that may indicate the presence of a small amount of a mixed layered illite-smectite. In both silty clays, glycolation of the samples shows some minor shifting to higher angles of the broad reflections in the 6-8°2θ region further suggesting the presence of a smectite component.

Figure 10 compares the particle size distribution of the 15 – 250 µm fraction of quartz calculated from the QEMSCAN® data with the same size fraction in the upper and lower silty clays measured by Malvern Mastersizer. Quartz is the dominant grain type in the iron ore, and therefore a comparison on a size for size basis with the grains in the silty clays, in which quartz grains again are dominant, would seem reasonable. Absolute amounts are not the same, and would not be expected to be, as the measurement parameters are different (linear % for the QEMSCAN® and volume % for the Malvern Mastersizer). However, the distributions are broadly similar with the dominant sizes being in the range 20-50 µm. This suggests that the quartz grains in the iron ore are identical to those within the clayey silts. Precipitation of the iron ore, therefore, has occurred around the pre-existing grains in the upper clayey silt. The larger sizes present in the clayey silt, but absent in quartz measured by QEMSCAN®, are probably larger composite grains of more than one mineral from gabbro, or liberated coarse crystals from the gabbro incorporated into the clayey silt. Grains identified as pyroxene / amphibole in the QEMSCAN®, presumably from the gabbro, were also in the range 60-250 µm.

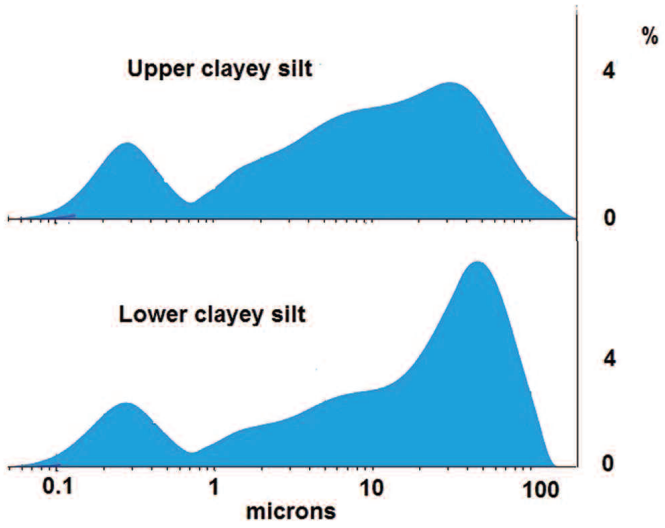

Figure 8. *Particle size distributions of <250 µm fractions of the upper and lower clayey silts.*

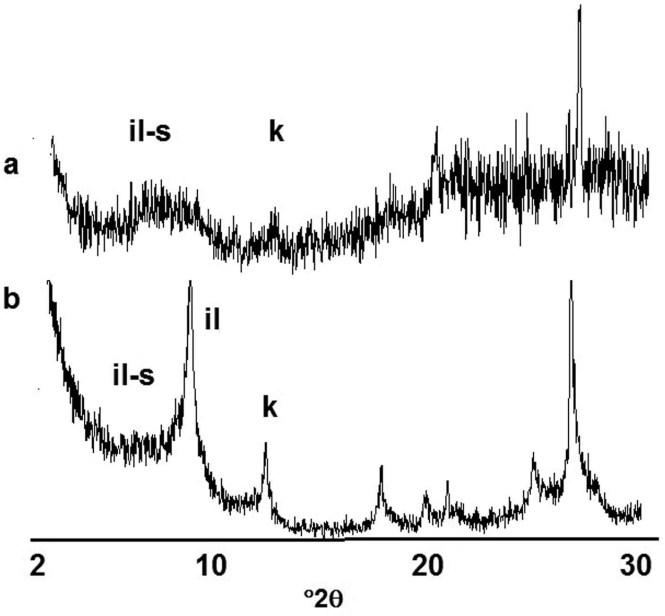

Figure 9. *X-ray diffraction patterns of <2 µm fractions of upper (**a**) and lower (**b**) clayey silts. Symbols: il – illite, il-s – illite-smectite, k – kaolinite. 2θ scale for CuKα radiation.*

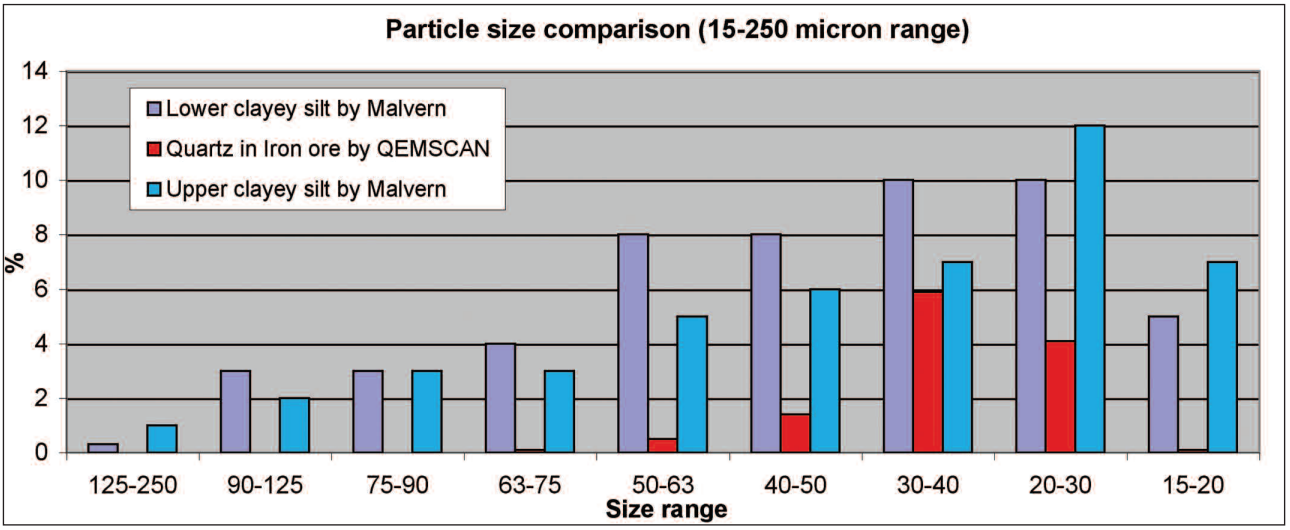

Figure 10. *Comparison of particle size distribution of quartz grains determined from the QEMSCAN® data with grains of the same size range from the upper and lower silty clays determined using the Malvern Mastersizer.*

Discussion

The geological setting of the iron ore is illustrated as a cartoon in Figure 11. An impermeable plastic clayey silt made up of quartz and other grains of loessic origin in a matrix of dominantly illite and kaolinite clay minerals accumulated on top of a weathered gabbro surface. The gabbro, which does not contain significant amounts of quartz and would most likely weather initially to a smectite-rich clay followed by kaolinite but not illite, does not appear to have been the major source of the loess or clay. Catt and Staines (1982) proposed a source for the loess in Cornwall from the Late Devensian outwash deposits from the Irish Sea Basin, and not from weathered local Variscan granites. However, either of these sources would fit with the observed mineralogy of the lower clayey silt.

Relatively clay-free (i.e. non-plastic) and free-draining loess occurs beneath the soil horizon to the south of the area with the clayey silt, large gabbro boulders and iron ore. The relationship between this loess and the lower clayey silt is transitional. Therefore, it is possible that the lower clayey silt is the same loessic material re-worked and/or simultaneously accumulating in water, perhaps a shallow partly drying lagoon, in which clay particles would also collect. Dessication of the silty clay in a 'drying' lagoon could also account for the observed mottling.

Large gabbro boulders, only found on the foreshore immediately in front of the area of the iron ore, accumulated on top of the clayey silt and most likely pressed into it because of their weight. Their size and restricted distribution is such that they do not appear to have been moved any significant distance by wave action. They cannot be *in situ* residual boulders of gabbro from weathering as they do not appear to rest directly on top of the weathered gabbro bedrock. They may, therefore, represent the remains of a periglacially degraded cliff, smaller boulders, cobbles and finer material having been removed by the sea. The presence of broken boulders, probably fractured by frost action, with the fractures partly infilled with iron ore and clayey silt, suggests that the age of the boulders is not recent.

The upper clayey silt at the base of the soil profile, also contains loessic material along with some very poorly crystalline clay. It is slightly porous, as there is water seepage at its base. It will have surrounded or covered the large gabbro boulders now present on the foreshore, and along with the remainder of the soil, most likely covers or surrounds other similar boulders inland towards the palaeo-cliff. The top surfaces of similar sized large boulders are present behind the present-day low cliff. The contact between these boulders and the upper clayey silt would be a pathway for water which would migrate through the upper clayey silt and between the boulders along the top surface of the lower impermeable clayey silt. This is the horizon at which the iron ore has accumulated.

The field relations, petrography and mineralogy of the ores show that precipitation of iron and manganese oxides took place within a clayey silt of loessic origin, particularly where it is in contact with the large gabbro boulders. Precipitation of the ore mostly took place at the interface between the two clayey silts, the iron and manganese minerals surrounding and incorporating the quartz and other silt grains and clay particles of one or other or both of the silty clays. The precipitation of iron and manganese oxides took place simultaneously and separately as distinct Fe oxide, Mn oxide and mixed Fe-Mn oxide concentrations are present.

A genetic model for the bog iron ore

A general model for bog iron ore formation involves low pH reducing conditions in surface waters or in the vadose zone caused by decaying organic matter that mobilise iron as soluble Fe^{2+}. Interaction with more free-flowing oxygenated groundwater causes oxidation of the iron, which precipitates as poorly crystalline Fe^{3+} iron oxides and hydroxides, sometimes

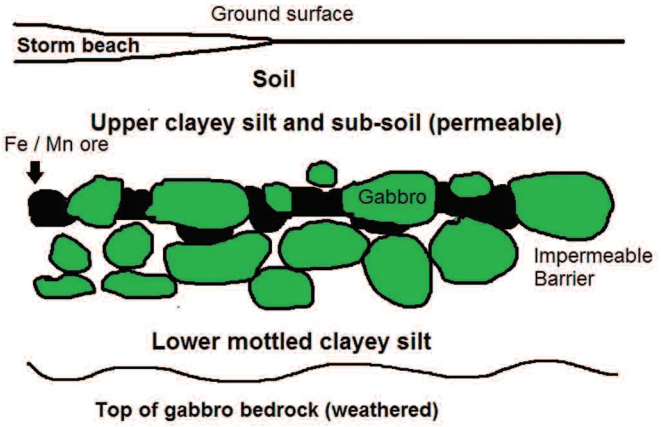

Figure 11. *Cartoon showing geological setting of the bog iron ore.*

called 'limonite', along the water table (Stanton 1972). The product is grains, discs or sometimes more extensive lenses and layers of iron oxides, which wholly or partly recrystallises to form goethite, mixed with clay and other fine detritus. This model would appear to be generally applicable for the present situation, except that the presence of manganese requires additional explanation, and the absence of a clearly defined water table and the position next to the sea perhaps leads to a different interpretation of the precipitation mechanism.

The source of the Fe and Mn is almost certainly from dissolution through extended weathering of the gabbro in the Lizard plateau area that extends for several kilometres behind the present palaeo-cliff. The presence of 'crusairs' (residual boulders of gabbro) on the plateau and a thick weathering profile in excess of 15 m in the overburden of the adjacent Dean Quarry is confirmation that such deep chemical weathering and dissolution has occurred.

There is no permanent surface stream in the area of the bog iron ore. Groundwater flow, therefore, is the dominant discharge mechanism draining the Lizard Plateau in this area. Precipitation of Fe and Mn would occur in response to oxidation as groundwater comes towards the surface in the area of the shoreline cliffs (Krauskopf and Bird, 1995), perhaps aided by the presence of oxidising bacteria. Although there is no direct evidence here, biomineralisation is a probable mechanism for iron ore formation in similar settings (e.g. Wu *et al.*, 2009). Precipitation would also occur as a consequence of an increase in pH due to the marine setting, sea water from storms and salt spray percolating into the soil and mixing with the groundwater. Precipitation of Fe and Mn oxides and hydroxides, which cement pebbles at the base of the raised beach at Godrevy on the north coast of Cornwall (Hosking and Pisarski, 1964), similarly has been attributed to increase in pH from contact with seawater.

The QEMSCAN® data shows partial segregation of Fe and Mn in the ore with precipitation of either or both elements within different parts of the ore. The Eh – pH ranges for dissolution and precipitation of Fe and Mn are similar, but as Mn dissolves over a wider range of Eh and pH, and can remain in solution when Fe is precipitated (Stanton, 1972; Krauskopf and Bird, 1995), the observed segregation is to be expected. Fluctuations in Eh and/or pH either during dissolution or precipitation will encourage mobilisation or deposition of one element at the expense of the other, further promoting segregation.

This is the first reported occurrence of iron ore of this type in Cornwall. Although it is found at and near the surface, there is no known association between the ore as a source of iron and the extensive archaeological record of the area.

ACKNOWLEDGEMENTS

Rev. Vincent Holyer first drew our attention to this unusual mineralisation at Polcries. The authors acknowledge assistance from the Camborne School of Mines technical staff, namely Steve Pendray who made the polished blocks and polished thin sections, Fiona Downey who carried out the XRF chemical analyses, and Robert Fitzpatrick who completed the particle size measurements and <2 µm size separation.

REFERENCES

BATES, R. and SCOLDING, B. 2000. Beneath the skin of the Lizard. Cornwall County Council.

BUDGE, E. 1842. On the tract of land called the Lowlands in the Parish of St Keverne. *Transactions of the Royal Geological Society of Cornwall*, **6**, 59-63.

CATT, J.A. and STAINES, S.J. 1982. Loess in Cornwall. *Proceedings of the Ussher Society*, **5**, 368-375.

EALEY, P.J. and JAMES, H.C.L. 2011. Loess of the Lizard Peninsula, Cornwall, SW Britain. *Quaternary International*, **231**, 55-61.

FLETT, J.S. 1946. *Geology of the Lizard and Meneage, 2nd Edition*. Memoir of the Geological Survey of Great Britain. HMSO.

FLOYD, P.A., EXLEY, C.S. and STYLES, M.T. 1993. *Igneous rocks of south-west England*. Joint Nature Conservancy Committee and Chapman and Hall, London.

GOTTLIEB, P., WILKIE, G., SUTHERLAND, D., HO-TUN, E., SUTHERS, S., PERERA, K., JENKINS, B., SPENCER, S., BUTCHER, A. and RAYNER, J. 2000. Using quantitative electron microscopy for process mineralogy applications. *Journal of the Minerals, Metals and Materials Society*, April 2000, 24-25.

KRAUSKOPF, K.B. and BIRD, D.K. 1995. *Introduction to geochemistry,* 3rd Edition. McGraw – Hill Inc., New York.

HOSKIN, K.F.G. and PISARSKI, J.B. 1964. Chemical characteristics of the cements of the Godrevy 10-ft raised beach and of certain deposition pipes in the St Agnes Pliocene deposits, Cornwall. *Transactions of the Royal Geological Society of Cornwall*, **19**, 328-348.

PIRRIE, D., BUTCHER, A.R., POWER, M.R., GOTTLIEB, P. and MILLER, G.L. 2004. Rapid quantitative mineral and phase analysis using automated scanning electron microscopy (QEMSCAN®); potential applications in forensic geoscience. In PYE, K. and CROFT, D.J. (Eds.), *Forensic Geoscience, Principles, Techniques and Applications*. Geological Society, London, Special Publication, **232**, 123-136

ROLLINSON, G., ANDERSEN, J.C.Ø., STICKLAND, R.J., BONI, M. and FAIRHURST, R. 2011. Characterisation of non-sulphide zinc deposits using QEMSCAN®. *Minerals Engineering,* **24**, 778-787.

STAINES, S.J. 1984. *Soils in Cornwall III, Sheet SW61/62/71/72 (The Lizard)*. Soil Survey Record No 79.

STANTON, R.L. 1972. *Ore Petrology*. McGraw-Hill Inc.

WU, Z., YUAN, L., JIA, N., WANG, Y. and SUN, L. 2009. Microbial biomineralization of iron seepage water: Implication for the iron ores formation in intertidal zone of Zhoushan Archipelago, East China Sea. *Geochemical Journal*, **43**, 167-177.